Journal of Catalysis 266 (2009) 1–8

Contents lists available at ScienceDirect

Journal of Catalysis

journal homepage: www.elsevier.com/locate/jcat

Investigation of the catalytic activities of sulfated mesoporous Ti, Nb, and Ta oxides in 1-hexene isomerization

Yuxiang Rao [a], Junjie Kang [a], Michel Trudeau [b], David M. Antonelli [a,*]

[a] Department of Chemistry and Biochemistry, University of Windsor, 401 Sunset Avenue, Windsor, Ontario, Canada N9B 3P4
[b] Chemistry and Materials, Hydro-Québec Research Institute, Varennes, Quebec, Canada J3X 1S1

ARTICLE INFO

Article history:
Received 6 January 2009
Revised 24 April 2009
Accepted 10 May 2009
Available online 9 July 2009

Keywords:
Mesoporous Ti oxide
Mesoporous Nb oxide
Mesoporous Ta oxide
1-hexene isomerization
Ligand-assisted amine templating approach
Confinement effect

ABSTRACT

In the present work, a series of porous transition metal (Ti, Nb, and Ta) oxides with different pore sizes (12–30 Å) were synthesized using a ligand-assisted amine templating approach. The as-synthesized samples were further treated with 1M sulfuric acid and were characterized by nitrogen adsorption/desorption, powder X-ray diffraction (PXRD), Fourier transform infrared spectroscopy (FTIR), high-resolution transmission electron microscopy (HRTEM), scanning electron microscopy (SEM), thermogravimetric analysis (TGA), differential scanning calorimetry (DSC), and elemental analysis (EA). The experimental results in the isomerization of 1-hexene were compared with the commercially available zeolites (HY-zeolite and H-ZSM5) and the ion exchange resin Amberlyst 15. The best results were achieved when using $C_{12}H_2SO_4$ mesoporous Ta oxide, which possesses a Ho of −8.2 and 19.8 mmol g^{-1} acid sites. The conversion of 1-hexene to trans/cis 2-isomers reaches 95.89% in 4 h and the ratio of trans/cis isomers reaches up to 3.7 after 6 h, which is very close to their theoretical ratio in thermodynamic equilibrium (3.37) under the same conditions. This conspicuously high selectivity and short reaction time were not detected with the Ta materials synthesized with C_{18} or C_6 templates, nor with Ti and Nb materials of any pore size under the same reaction conditions. Temperature-programed desorption (TPD) of ammonia was used to investigate the much higher activity of the Ta materials. The results showed that the Ta materials had a much greater concentration of Brønsted sites in the active *Ho* range for this reaction than the Nb materials. The unique performance of the $C_{12}H_2SO_4$ Ta material was thus attributed to its high BET surface area, increased concentration of effective Brønsted acid sites and optimal pore size for this particular reaction.

1. Introduction

Over the last two decades, there has been a dramatic increase in the synthesis of open-framework micro- and mesoporous inorganic materials of well-defined pore geometry. One of the most important classes of these materials is the M41S family of mesoporous silicates, first synthesized by Mobil Corporation in 1992 [1,2]. Since that discovery, there has been considerable interest in exploiting their unique properties, which include controlled pore sizes, high surface area, and high thermal stability, which are all areas of great importance to catalysis and gas separation [3,4]. One of the most important potential applications of these materials is in acid-catalyzed petroleum and hydrocarbon transformations [5–7], because the larger pores are thought to be an advantage in the suppression of coking. However, mesoporous aluminosilicates do not possess high enough acidities to be useful in many of these reactions. For this reason there has been considerable interest in synthesizing mesoporous materials from highly acidic transition metal oxides and their sulfated analogues. Since the first report of the synthesis of non-silica transition metal oxide mesoporous materials, accomplished using a ligand-assisted templating approach for Nb, Ta, and Ti [8–12], many groups have begun to investigate the catalytic properties of these and related materials. Thus, a wide variety of mesoporous transition metal oxides have been reported as novel catalyst materials [13,14]. Mesoporous transition metal oxides have superior properties in many applications as compared to their traditional silica analogues due to their high acidities and the variable oxidation states afforded by the empty transition metal d orbitals, which allow electron transfer to occur between the reactants and active sites during any given catalytic process [15,16]. Recently, we showed that sulfated mesoporous Nb and Ta oxides possess a high concentration of Brønsted acid sites, useful in Friedel Crafts reactions such as benzylation [17] and alkylation [18]. Mesoporous Ta oxide is also an very effective catalyst in the isomerization of 1-hexene, surpassing both zeolite Y and Amberlyst 15 in activity and selectivity [19]. In this report, we present a detailed comparative study of the reaction of 1-hexene over a series of sulfated mesoporous Ti, Nb, and Ta

* Corresponding author. Fax: +1 5199737098.
E-mail addresses: rao7@uwindsor.ca (Y. Rao), danton@uwindsor.ca (D.M. Antonelli).

0021-9517/$ - see front matter © 2009 Elsevier Inc. All rights reserved.
doi:10.1016/j.jcat.2009.05.014

catalysts with different pore sizes and compare their activity to standard zeolites and ion exchange resin Amberlyst 15. The relative activities of the Nb and Ta materials are also studied by temperature programed desorption of ammonia in order to establish the reason for the much higher activity of the Ta-based system in this model reaction (see Table 1).

2. Experimental

2.1. Materials

All chemicals unless otherwise stated were obtained from Alfa Aesar without further purification. HY zeolite and HZSM5 were purchased from Zeolyst, and Amberlyst 15 was purchased from Aldrich.

2.2. Synthesis of sulfated mesoporous titanium, niobium, and tantalum oxide materials with different pore sizes

Mesoporous titanium and niobium oxides were prepared according to the literature [8,12]. In a typical preparation, niobium ethoxide (50 g, 157.1 mmol) was warmed with *n*-dodecylamine (8.7372 g, 47.13 mmol) (*n*-hexylamine for C_6Nb and *n*-octadecylamine for C_{18}Nb) using a heat gun until a homogeneous colorless solution was obtained. To this solution was added 1 L of distilled water with stirring. A white gelatinous precipitate formed immediately. After precipitation occurred, hydrochloric acid (37%, 0.1743 g, 4.713 mmol) was added directly to the solution without agitation before the white solid was allowed to sit at room temperature overnight. The mixture was heated at 40 °C for 2 days, 60 °C for 2 days, 80 °C for 2 days, and 95 °C for 4 days. After filtration, the solid was dried in an oven at 95 °C for 1 ∼ 2 h, sealed in a tube, and heated to 120 °C for 2 days and 140 °C for 2 days. The product was then collected and washed five times with 500 ml of methanol to remove the surfactant. Each washing cycle was conducted for 24 h in a large Erlenmeyer flask with vigorous stirring followed by filtration. For the first wash, p-toluene sulfonic acid (9.8615 g, 51.843 mmol) was added to the solution with 200 ml diethyl ether. For the second washing, 0.8965 g p-toluene sulfonic acid was added to methanol solution. After 5 washings the solid was collected and dried for 24 h at 120 °C. The template-free sample was further treated with 1 M sulfuric acid solution (in methanol) for 24 h and filtered in vacuum for another 24 h. Later, the samples were heated to 120 °C at 10–3 Torr overnight to evaporate the solvent remaining in the pores and obtain the sulfated mesoporous Nb oxides (Scheme 1). The synthesis for mesoporous Ti and Ta oxides is identical, except that the Ti sample was removed from water at 80 °C to avoid hydrothermal structure collapse and then aged dry up to 120 °C for 5 days before the removal of template. Also, Titanium isopropoxide and tantalum ethoxide are used in place of niobium ethoxide, respectively, in these cases. The samples were characterized without any further treatment.

Table 1
Acid strength and acid amount of solid acid catalysts (measured by Hammett indicators and *n*-butylamine titration).

Sample	*Ho*	Acid amount (mmol g^{-1})
C_{12} Meso Ti	+3.3	2.0
C_{12} H_2SO_4 Meso Ti	+0.8	4.7
C_{12} Meso Nb	−6.6	2.4
C_{12} H_2SO_4 Meso Nb	−8.2	31.7
C_{12} Meso Ta	−6.6	0.4
C_{12} H_2SO_4 Meso Ta	−8.2	19.8
HY Zeolite	−6.6	1.5
H-ZSM5	−4.4	16.1
Amberlyst 15	N/A	N/A

2.3. Instruments and characterization

Nitrogen adsorption and desorption data were collected on a Micromeritics ASAP 2010. X-ray diffraction (XRD) patterns (Cu Kα) were recorded in a sealed glass capillary on a Siemens D-500 θ–2θ diffractometer. High-resolution transmission electron microscopy (HRTEM) images were obtained by using H9000 HR-TEM operated at 300 kV. Scanning electron microscopy (SEM) images were recorded on S-4700 Cold Field Emission SEM from Hitachi. Pyridine adsorption Fourier transform infrared spectroscopy (FTIR) experiments were performed on Bruker Vector 22 FTIR spectrometer after evacuation at room temperature and 10^{-3} Torr. TGA and DSC data were collected on a TGA/SDTA851 (Mettler Toledo) with Pfeiffer Vacuum Thermostar and DSC822E Differential Scanning Calorimeter (DSC) (Mettler Toledo), respectively, from room temperature to 550 °C at a heating rate of 5 °C min^{-1}. TPD experiments were conducted on a ChemBET TPR/TPD instrument from Quantachrome using ramp rates of 5 K/min, 10 K/min, and 20 K/min. All elemental analysis data (conducted under an inert atmosphere) were obtained from Galbraith Laboratories, Knoxville, TN.

2.4. Thermodynamic equilibrium constant measurement

The thermodynamic equilibrium constant was calculated using the standard Gibbs energy equation

$$\Delta G^{\Phi} = -RT \ln K_{eq} \quad (1)$$

where ΔG^{Φ} is the standard Gibbs energy change of reaction, R is the gas constant, and T is the absolute temperature. From Ref. [20], we know that $G_{\text{cis-2-hexene}} = 19.18$ kcal mol^{-1} and $G_{\text{trans-2-hexene}} = 18.46$ kcal mol^{-1}, so for the reaction cis-2-hexene → trans-2-hexene, $\Delta G < 0$. It is therefore a spontaneous reaction and trans-2-hexene is more stable than its cis-isomer. Inputting the numbers into Eq. (1) and use 343 K as the reaction temperature, we calculated the equilibrium constant $K_{eq.}$

2.5. Catalytic runs

A 100 ml round-bottomed three-necked flask equipped with a reflux condenser was used as a stirred batch reactor to test the catalytic activities of the materials. Nitrogen was introduced into the flask through one of the gas inlets. The second inlet was equipped with a septum for sample removal. 50 ml of 1-hexene (97%, Aldrich) were added to the reactor with 0.5 g catalysts at each run. The reactant mixture was refluxed with stirring at atmospheric pressure and constant temperature (controlled oil bath temperatures of 343 K) during the entire process, around 7 h at each run. Samples of the reaction mixture were periodically withdrawn and analyzed using a Varian CP-3800 gas chromatograph equipped with a hydrogen flame ionization detector system and capillary column CP-SIL 5CB (15 m, 0.25 mm ID), the temperature was programmed from 50 °C to 300 °C (10 °C/min) with H_2 1 ml/min as a carrier gas. Compared with a standard sample, the results from the GC identified trans-2-hexene and cis-2-hexene as the two main products. Activities were calculated on the basis of percentage conversion of 1-hexene in the starting mixture.

3. Results and discussion

The as-synthesized sulfated Ti, Nb, and Ta oxide samples were characterized by a series of standard analytical techniques (nitrogen adsorption and desorption, XRD, TEM, SEM, FTIR, Amine titration, TPD, TG, and DSC) prior to use as catalysts for the isomerization of 1-hexene. The results of these studies are detailed below.

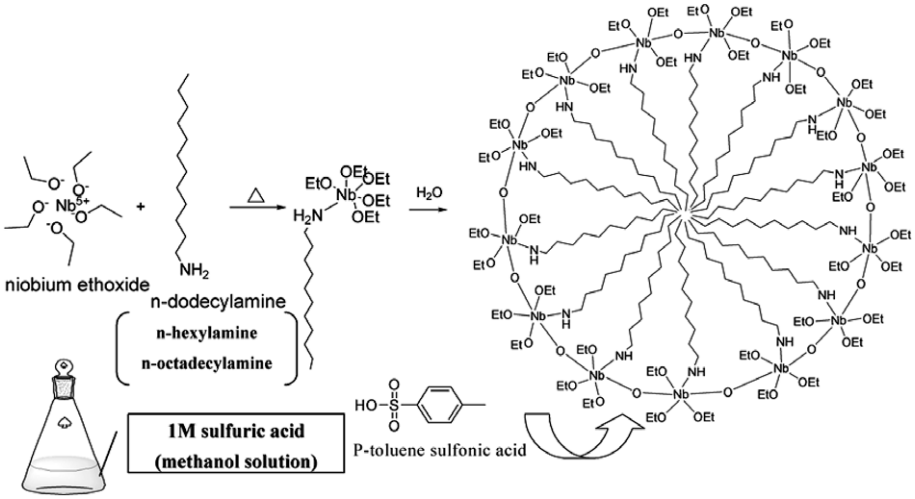

Scheme 1. Synthesis of sulfated mesoporous Nb or Ta oxide materials with different pore sizes.

3.1. XRD and nitrogen adsorption

The powder XRD patterns of the Ti, Nb, and Ta oxide samples before and after acid treatment were obtained to gain information about the mesoporosity and the effect of acid treatment on the stability of the mesoporous structure. While Nb_2O_5 and Ta_2O_5 are extremely robust to acid, the more loose-knit gel structure of the mesostructure walls in these materials is expected to lead to lower kinetic and thermal stabilities. ^{17}O NMR experiments conducted by our group showed that mesoporous Nb oxide possesses almost exclusively 2-coordinate oxygen, with only very small amounts of triply bridging oxygen, which was confirmed by a weak side peak at 350 ppm on the ^{17}O MAS NMR spectra of ^{17}O-enriched mesoporous Nb [21]. This would facilitate any acid-catalyzed hydrolysis reactions that could lead to structural degradation of the walls. Nevertheless, X-ray diffraction (XRD) analysis of the powder samples in Fig. 1 clearly showed that the mesoporous structures are retained after acid treatment, as the main peak at low angle in each sample representing the strong reflection (1 0 0) is almost unchanged. This was further confirmed by the type IV isotherm obtained by the nitrogen adsorption/desorption measurement in Fig. 2. However, the BET surface area and the BJH pore sizes of mesoporous Ti, Nb, and Ta oxides decreased after acid treatment (Table S1), possibly due to the deposit of SO_4^{2-} ions inside the wormhole channels which would lead to an increase of skeletal density and a concomitant loss of void space, effectively lowering the surface area per gram (Figs. 1, 2, Table S1).

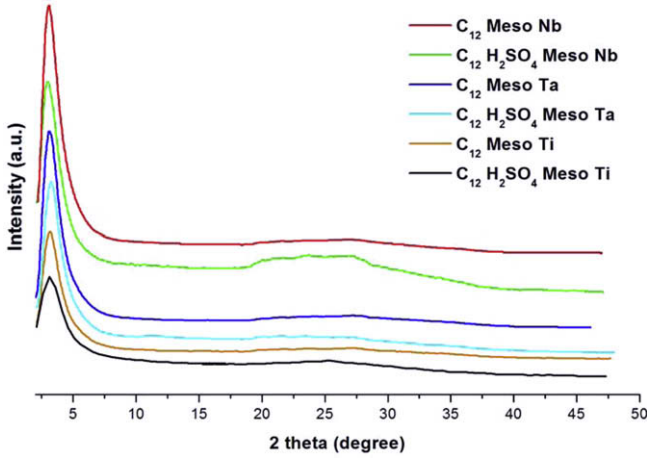

Fig. 1. Powder X-ray diffraction data for Nb-TSM1, Ta-TSM1, and Ti-TSM1 samples. (From Top to Bottom) (a) C_{12} Meso Nb; (b) C_{12} H_2SO_4 Meso Nb; (c) C_{12} Meso Ta; (d) C_{12} H_2SO_4 Meso Ta; (e) C_{12} Meso Ti; and (f) C_{12} H_2SO_4 Meso Ti.

3.2. TEM and SEM images

TEM and SEM images of C_{12} mesoporous Ti, Nb, and Ta samples were obtained (Fig. 3) to elucidate the structure and morphology of these materials. TEM images of Ti, Nb, and Ta samples (Fig. 3b,d, f) clearly indicate the formation of an ordered mesostructure with a disordered arrangement of mesoporous channels. The C_{12}Ti, Nb and Ta materials possess a powder morphology with a large range of particle sizes from several hundred nanometers over 100 μm. These images are virtually identical to those of unsulfated Nb and Ta materials synthesized by our group and thus confirm that sulfuric acid treatment had little effect on the overall mesostructure or particle morphology of these samples.

3.3. FTIR of pyridine adsorption spectra

The FTIR (Fourier transform infrared, Fig. 4) spectrum of C_{12} mesoporous Nb oxide treated with pyridine vapor showed that Brønsted (1540 cm^{-1}) and Lewis (1450 cm^{-1}) acid sites coexist on the surfaces of the parent material. However, both the sulfated Nb and Ta materials exhibited a strong dominance of Brønsted acid sites, which is the result of sulfuric acid treatment. The FTIR data for mesoporous Ta oxide have been published previously, and show the same trend in increased Brønsted acid sites with sulfuric acid treatment [18]. The majority of research indicates that Brønsted acid sites are chiefly involved in isomerization reactions [23–25], which should give these sulfated Nb and Ta materials a distinct advantage in these reactions. In contrast, although HY-Zeolite and H-ZSM5 were preheated to 500 °C for 3 h to remove the surface water before pyridine adsorption, by our measurements these materials possess mainly Lewis acid sites (~1448 cm^{-1}) with only a weak absorbance observed for Brønsted acid sites.

3.4. Amine titration and TPD experiments

Hammett acidity and *n*-butylamine titration methods were employed as reported to measure the acid strength and acid amount of all samples [26]. The experimental results are summarized in Table S1. As seen from this table, both the acid strength and acid

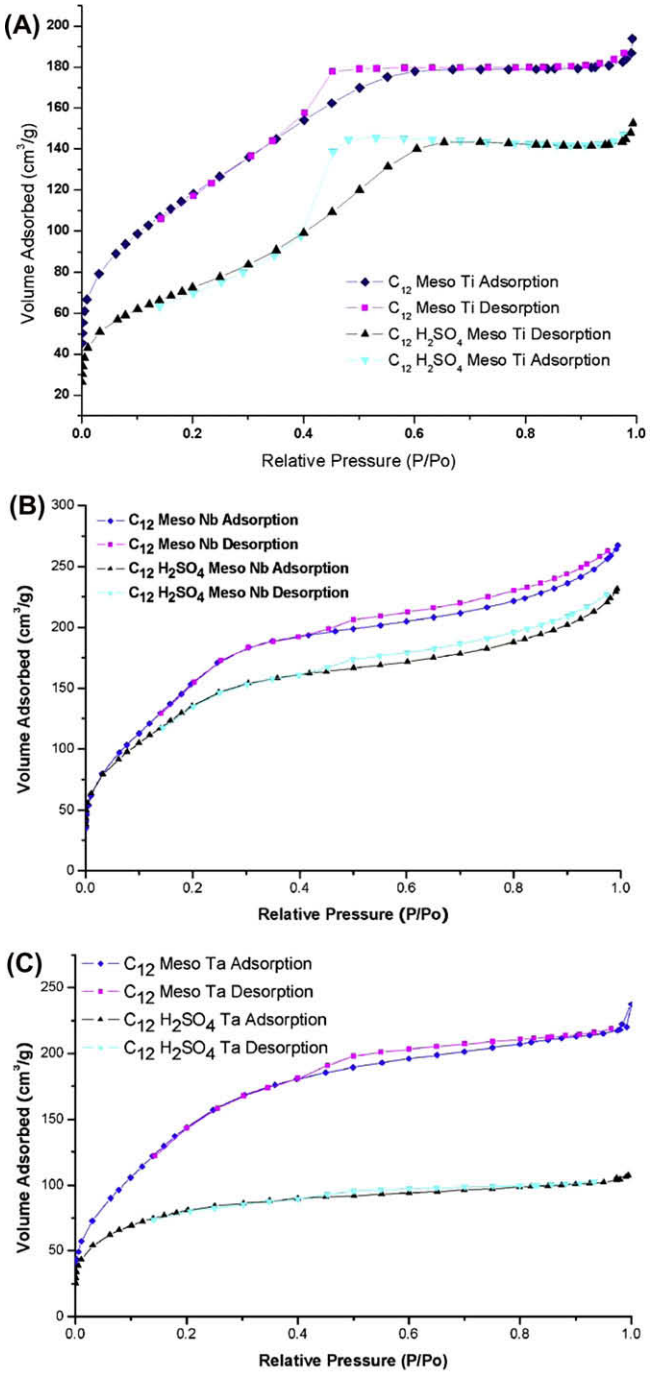

Fig. 2. N_2 adsorption/desorption isotherm of (a) C_{12} Meso Ti and C_{12} H_2SO_4 Meso Ti; (b) C_{12} Meso Nb and C_{12} H_2SO_4 Meso Nb; and (c) C_{12} Meso Ta and C_{12} H_2SO_4 Meso Ta.

amount of the C_{12}Nb and Ta oxides increase dramatically after acid treatment, consistent with the previous work on the benzylation of toluene and anisole by C_{12} mesoporous Nb oxide [17]. In contrast, the C_{12}Ti sample possesses a relatively weak acid strength ($Ho \sim +3.3$) and low acid amount of 2.0 mmol g^{-1} in pristine form. The acid strength of this material increases only slightly to $Ho \sim +0.8$ and 4.7 mmol g^{-1} after treatment with sulfuric acid. This suggests that although the surface area for mesoporous Ti oxide may be higher than that for the Nb and Ta counterparts, the catalytic activity may not be as high in reactions requiring stronger acid sites. The values of 31.7 mmol g^{-1} and 19.8 mmol g^{-1} for C_{12} sulfated mesoporous Nb and Ta are quite high when compared to the samples of bulk sulfated zirconias (2.23 mmol g^{-1}) [27], but the differences in surface areas between these materials or the inherent accuracy limitations of this method may account for this difference (413.97 m^2 g^{-1} for $C_{12}H_2SO_4$ Meso Nb and 292.19 m^2 g^{-1} for $C_{12}H_2SO_4$ Meso Ta vs. 60 m^2 g^{-1} for sulfated zirconia). Since C_{12} sulfated mesoporous Nb and Ta samples were dried in vacuum for 24 h and then pre-heated at 10^{-3} Torr at 120 °C for 24 h to evaporate the remaining solvent before titration, this rules out the possibility of residual liquid sulfuric acid in the mesopores influencing the acidity measurements. Because C_{12} sulfated mesoporous Nb and Ta oxides possess similar acid strength ($Ho \sim -8.6$) and acid amount (31.7 mmol g^{-1} for Nb and 19.8 mmol g^{-1} for Ta) as determined by this method, more detailed studies are required to account for their remarkable differences in catalytic activity observed between these two materials in the previous studies [19].

Temperature-programed desorption (TPD) is an excellent method to measure the relative strengths of acid sites in a material. Ammonia desorption is routinely used as a method to measure binding enthalpies and relative amounts for both Lewis and Brønsted sites [28–32], while Ar desorption can be used to measure Lewis acid strength of super acidic materials at low temperature [33,34].

For these experiments, sulfated mesoporous Nb and Ta oxides were first pre-heated to 500 °C to eliminate the surface water and other decomposable components before treatment with ammonia vapor for the TPD of ammonia experiments. TPD data for the desorption of ammonia from the C_{12}Nb and Ta catalysts are given in Fig. 5. The NH_3-TPD curve for $C_{12}H_2SO_4$Ta shows one intense and broad peak at 868 K (middle) and two smaller peaks at 802 K (first) and 1023 K (last), corresponding to one strong Brønsted acid site, one weak Lewis acid site and one strong Lewis acid site, respectively, as reported elsewhere [28,29]. In the previous studies on zirconia the intensity of this central Brønsted peak was associated with high activity in acid-catalyzed reactions [28–30]. The Nb sample has two main peaks at 840 K (Lewis acid site) and 909 K (Brønsted acid site), the other peak at high temperature (1033 K) is small compared to that in the curve for the Ta analogue. The main Nb Brønsted peak is lower in integrated intensity and also much sharper than that for Ta, typical of desorption from a more highly crystallized surface. Since the walls in mesoporous Nb oxide crystallize at lower temperatures than mesoporous Ta oxide [21], the sharpness of the middle peak on the NH_3-TPD curve for $C_{12}H_2SO_4$ Meso Nb is most likely due to crystallization during the heating process leading to ammonia desorption from a more highly ordered surface above the crystallization temperature.

NH_3-TPD kinetic runs at constant heating rates of 5 °C min^{-1}, 10 °C min^{-1}, and 20 °C min^{-1} gave activation energies of desorption (Ed) of 157 KJ mol^{-1} and 169 KJ mol^{-1}, respectively, for the central Brønsted peak in the Ta and Nb curves. These values are in reasonable agreement with those determined by ITPD (intermittent temperature-programed desorption) study on perovskites reported by Gaillard [35,36]. Since these values are very close to one another, the greater intensity of the Ta Brønsted peak, and not the difference in *Ho*, likely accounts for the greater activity of the Ta material in reactions involving Brønsted acid sites.

3.5. TGA and DSC experiments

TGA and DSC techniques were applied to study the thermal behaviors of Nb and Ta samples and further elucidate the temperature of crystallization in the Nb sample. The results are shown in Figs. 6 and 7. The first large endothermic peak on both the Nb and Ta DSC curves at around 373 K corresponds to the evaporation of the residual water. The DSC curve for $C_{12}H_2SO_4$ Meso Nb shows a

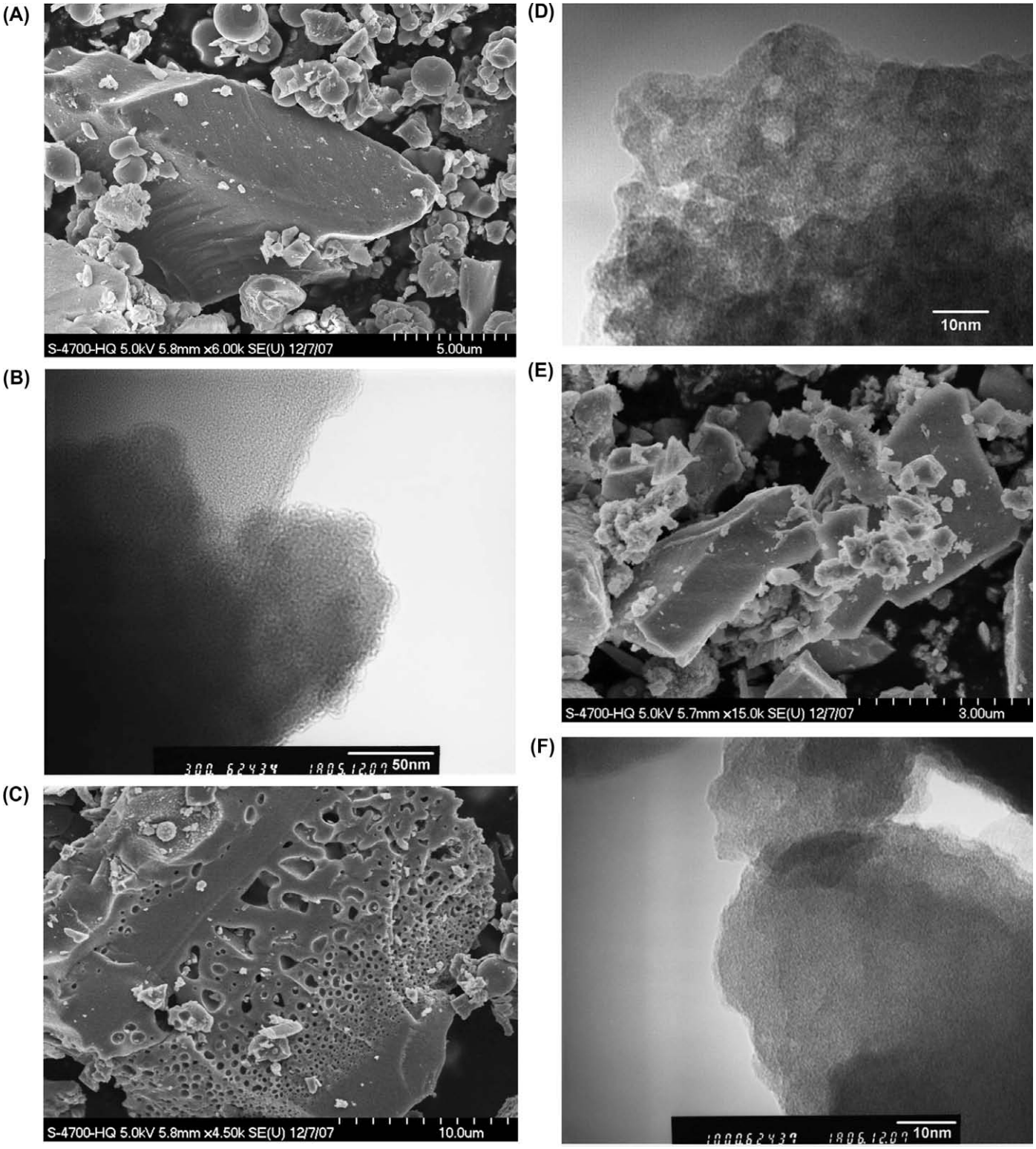

Fig. 3. (A) SEM images of the C_{12} H_2SO_4 Meso Ti. (B) TEM image of C_{12} H_2SO_4 Meso Ti. (C) SEM image of the C_{12} H_2SO_4 Meso Nb. (D) TEM image of C_{12} H_2SO_4 Meso Nb. (E) SEM image of the C_{12} H_2SO_4 Meso Ta. (F) TEM image of C_{12} H_2SO_4 Meso Ta.

large endothermic zone at 454–491 K, which can be attributed to the loss of structural water [37]. This is not found in the DSC curve for $C_{12}H_2SO_4$ Meso Ta. This is consistent with both previous XRD and ^{17}O NMR studies on mesoporous Nb oxide [21], and the observation of a very narrow peak in the TPD curve for the Nb sample.

3.6. Catalysts evaluation

Previous studies established that sulfated mesoporous Ta oxide was an effective catalyst in the isomerization of 1-hexene to the cis and trans 2-hexene products. GC analysis confirmed that trans and

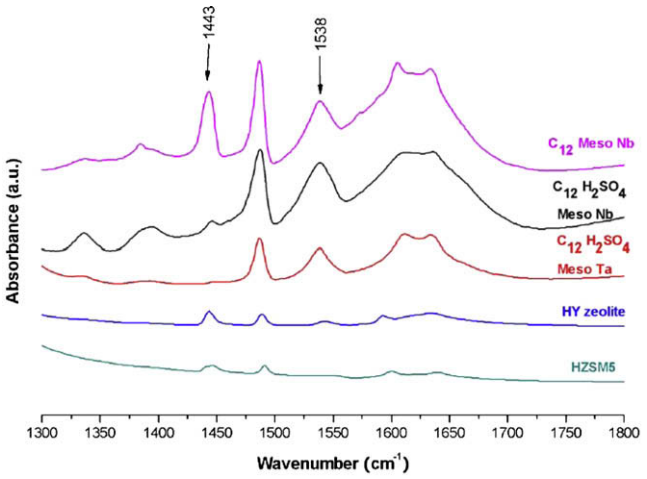

Fig. 4. FTIR of pyridine adsorption spectra on C_{12} Meso Nb, C_{12} H_2SO_4 Meso Nb and Ta, HY Zeolite and H-ZSM5 Zeolite.

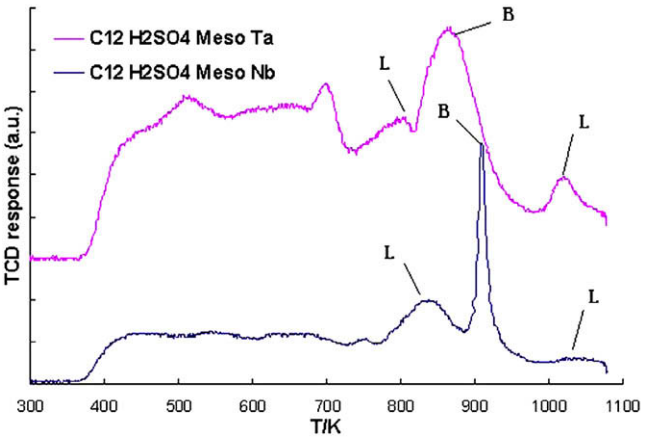

Fig. 5. NH_3-TPD profiles of sulfated mesoporous Nb and Ta catalysts. Ramp rate: 10 K min^{-1}.

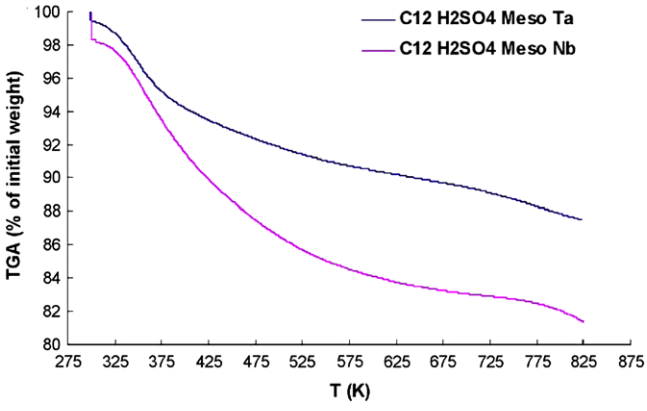

Fig. 6. TGA curves under N_2 for sulfated mesoporous Nb and Ta catalysts.

cis 2-hexene isomers were the only two products. Skeletal isomerization was not observed at this reaction condition since it requires more energy and can only be performed at elevated temperature (>523 K) [38–40]. In order to investigate the effect of pore size on the activity and selectivity toward trans-2-hexene in this reaction, a series of sulfated mesoporous Ti, Nb, and Ta oxides with

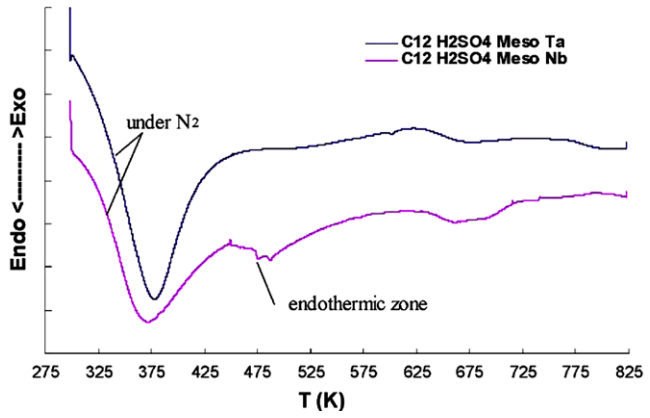

Fig. 7. DSC curves under N_2 for sulfated mesoporous Nb and Ta catalysts.

different pore sizes (C_6, C_{12}, C_{18}) were synthesized and then dried in vacuum at 10^{-3} Torr in 393 K for 24 h before measurement to make sure that there is no liquid sulfuric acid trapped in the pores. The samples were then evaluated for their catalytic activities at 343 K in a batch reactor. Commercially available zeolites (HY-zeolite and HZSM5) and the ion exchange resin Amberlyst 15 were chosen as reference catalysts. The Si/Al ratios for the HZSM-5 and HY Zeolite samples were 50 and 80, respectively, and these materials were pre-heated at 773 K for 3 h to activate before use. The results are shown in Figs. 8 and 9. The experiments were repeated at least twice using the same batch of catalyst but for the new reaction. The error bars reported are derived from true replicate experiments with 95% confidence intervals with +/−5% standard deviation.

Most likely due to its weak acidity and low acid amount, C_{12} sulfated Ti oxide only shows the relatively low catalytic activity of 29.4% conversion in 6 h, far lower than the Nb and Ta samples, but comparable to the zeolite materials in this study. The selectivity was also very similar to that of HY-zeolite. In general, C_{12} sulfated Nb and Ta samples possess higher activity and selectivity than their C_6 and C_{18} counterparts, which can be attributed to a combination of their relative higher BET surface area (413.97 m^2 g^{-1} for $C_{12}H_2SO_4$ Meso Nb and 292.19 m^2 g^{-1} for $C_{12}H_2SO_4$ Meso Ta; Table S1) and optimal pore size (18–20 Å). This is consistent with Tanchoux's observations on the higher activity of moderate pore size MCM-41 materials in the same reaction [41]. The author studied the impact of confinement and nesting effects in the isomerization of 1-hexene by MCM-41 and demonstrated that selectivity and conversion rate were pore size dependent. The conclusion was that both smaller pores and larger pores were less effective than moderately sized pores in this reaction.

Both the activities and selectivities of the Nb samples follow the order: $C_{12}H_2SO_4$ Meso Nb > C_{18} H_2SO_4 Meso Nb > $C_6H_2SO_4$ Meso Nb, (Fig 8a and b), matching the trend in their BET surface area (413.97 m^2 g^{-1} > 282.58 m^2 g^{-1} > 160.35 m^2 g^{-1}). $C_{12}H_2SO_4$ Meso Nb has the highest activity and selectivity, but it is only slightly higher than its C_6 counterpart. The conversion of 1-hexene to trans/cis 2-isomers reaches roughly 65% in 4 h and its trans/cis ratio can eventually reach 1.4 in 6 h. Although these three Nb samples showed a relatively large difference in activity (ranging from 40% to 85%), they all displayed a similar selectivity for this particular reaction (trans/cis ratio close to 1). The higher activities of all Ta materials relative to their higher surface area Nb counterparts can only be explained by the much more intense and broader distribution of Brønsted acid sites on the surface of Ta oxide relative to Nb oxide measured by TPD of ammonia experiments, as commented on above. (Fig. 5)

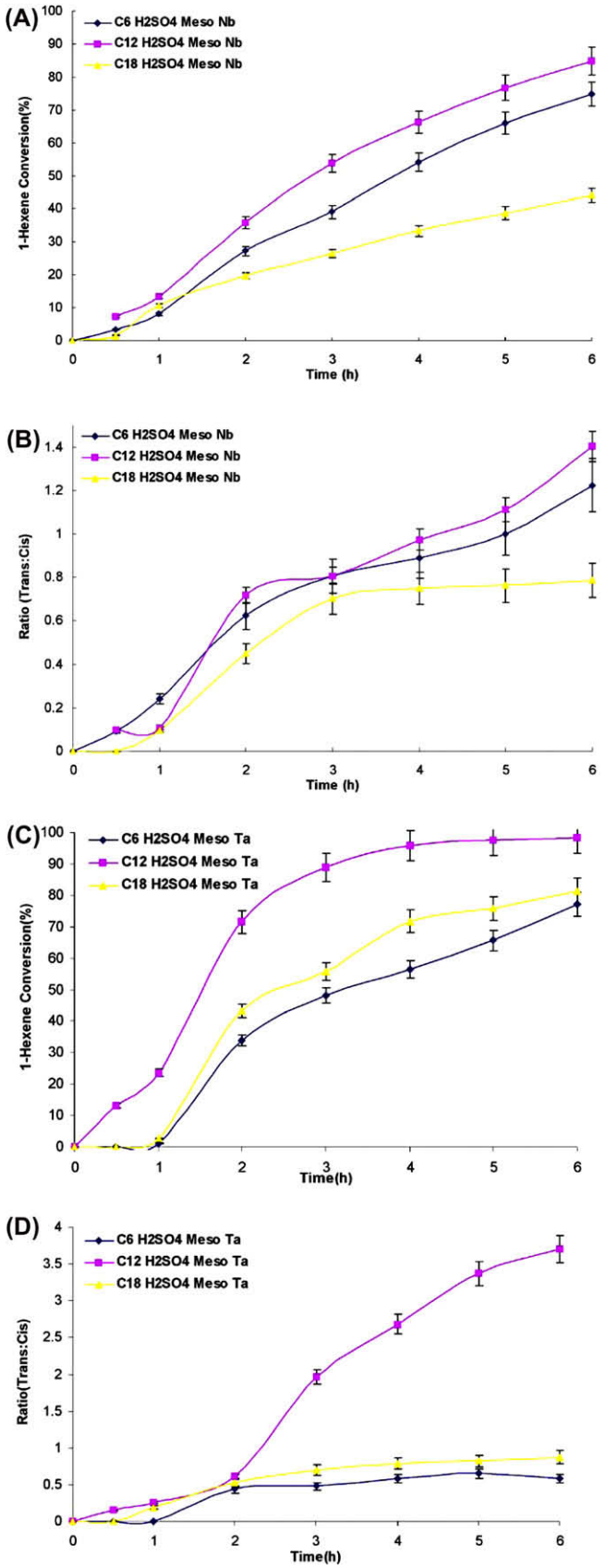

Fig. 8. 1-hexene isomerization conversion rate and selectivity on different pore size sulfated Nb and Ta oxides, (A) activity of different pore size Nb oxides, (B) selectivity of different pore size Nb oxides, (C) activity of different pore size Ta oxides, and (D) selectivity of different pore size Ta oxides.

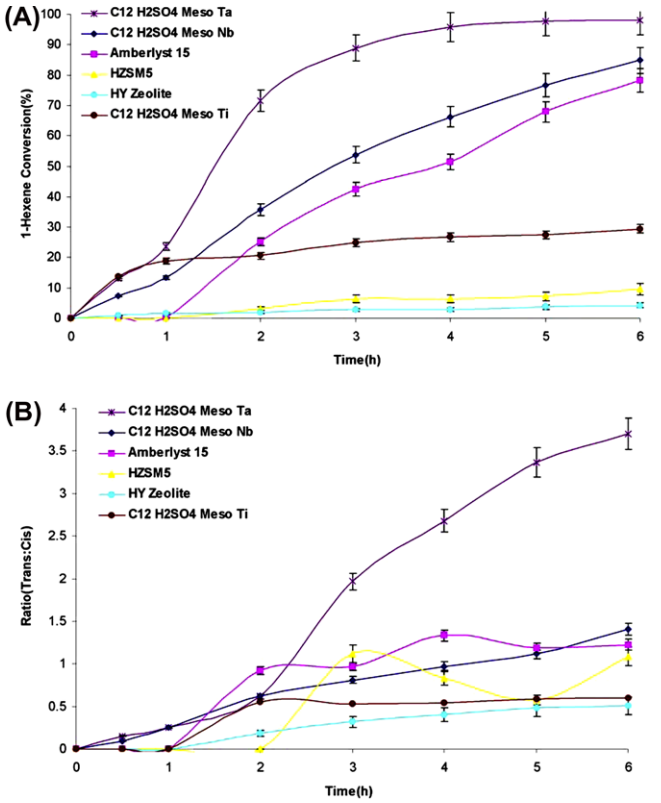

Fig. 9. 1-hexene isomerization conversion rate (A) and selectivity (B) on different catalysts.

The three different pore size Ta oxides samples (C_6, C_{12}, C_{18}) did not follow the same order. $C_6H_2SO_4$ Meso Ta has the smallest pore size (12 Å) and second highest surface area (206.40 $m^2\ g^{-1}$), but the lowest observed activity and second lowest selectivity. This can be explained by its much smaller pore size, which effectively hinders the free diffusion of the reactant (1-hexene in this reaction) and prevents access to the active Brønsted acid sites inside the pore, forcing most of the reaction to occur on the outer surface layer of the wall. This leads to both low activity and selectivity. In contrast, $C_{18}H_2SO_4$ Meso Ta possesses the largest pore size (22.5 Å), which allows the reactant (1-hexene) and products (both 2-hexene isomers) to diffuse in and out of its large pores without much hindrance. This leads to a poor selectivity. Although the large pore size of the C_{18} sample facilitates the diffusion of the reactant to the active site, this sample possesses the lowest surface area (188.79 $m^2\ g^{-1}$), which results in an activity that falls between that of its two congeners. $C_{12}H_2SO_4$ Meso Ta showed the highest activity (~95% in 4 h) and selectivity among these three Ta samples.

The moderate pore size of $C_{12}H_2SO_4$ Meso Ta oxide (18.2 Å, Table S1) also allows linear trans-2-hexene to pass more easily through its channels than non-linear cis-2-hexene. Its trans/cis ratio thus reaches 3.7 in 6 h, which is much greater than that in the other Nb and Ta samples which level off at a trans/cis ratio of close to 1. The trans/cis ratio for C_{12}Ta is very close to the thermodynamic equilibrium for this reaction (3.37) calculated using standard Gibbs energy equation. This increase in selectivity over time to the thermodynamic mixture can be attributed to the more efficient conversion of cis-2-hexene to trans-2-hexene in the pores of C_{12} Ta relative to the other catalysts (C_6 and C_{18}Ta) in this study. So, once the cis product is formed it is rapidly converted to the trans product, increasing the trans/cis ratio in the

reaction mixture. This material thus acts as a bifunctional catalyst, not only speeding up the 1-hexene isomerization conversion rates to the two isomers, but also facilitating the cis-2-hexene to trans-2-hexene isomerization in these two products. Abbot and Wojciechowski [42,43] systematically studied the isomerization reaction of 1-hexene to 2-hexene and reported that this reaction involves a proton transfer process, the initial proton is transferred from the acid sites on the surface of the catalyst to the double bond of 1-hexene, and then the hydride shift along the linear chain produces cis-2-hexene and trans-2-hexene. Further studies are necessary to investigate the confinement effect that results in the facile conversion of the two 2-hexene isomers after initial reaction.

The activity and selectivity of C_{12}Nb and Ta samples are compared with those of C_{12}Ti, HY zeolite, H-ZSM5, and Amberlyst 15 in Fig. 9. Both the Nb and Ta materials showed much higher activity than the C_{12}Ti and zeolites (HY zeolite and H-ZSM5) at this low reaction temperature (343 K), roughly 10 times greater and even higher than the well-known ion exchange resin Amberlyst 15, which is regarded as one of the best industrial catalysts for this reaction [42,43]. The selectivity of the C_{12}Ta material (3.7) toward trans-2-hexene is again superior to all other samples, which range from 0.5 to 1.1 after 6 h. Pure sulfuric acid was used as a reference catalyst in a separate experiment to eliminate the potential effect of free H_2SO_4 on selectivity [19]. The conversion of 1-hexene reached 31.18% after 6 h, and an only slightly higher product ratio (1.5) was obtained as compared to the C_6 and C_{18}Nb and Ta samples. This is still far behind the selectivity of $C_{12}H_2SO_4$ mesoporous Ta oxide, which establishes once again that pore size is crucial to the selectivity in this system.

To test the reusability of $C_{12}H_2SO_4$ mesoporous Ta, three continuous runs were conducted using the same catalyst. The results showed that catalytic activity declined linearly, the conversion rate of 1-hexene decreasing from almost 100% to 76%, and then to 40% [19]. This may be attributed to partial pore blockage caused by isomerization products deposited inside the channel. This is consistent with the drop in BET surface area from 292 $m^2 g^{-1}$ to 133.25 $m^2 g^{-1}$. However, elemental analysis shows no increase in %C under these mild conditions (343 K), demonstrating that the loss of surface area and activity is not due to the build up of carbon species. The activity of the used catalyst can be partially regenerated to 60% its original activity by treatment with new sulfuric acid, which shows that sulfate leaching during each catalytic run is at least partially responsible for the gradual loss of catalytic activity on recycling.

4. Conclusion

This paper provides a clear demonstration of the influence of acid sites and confinement effect in 1-hexene isomerization catalyzed over sulfated mesoporous Nb and Ta oxides. These catalysts showed higher activities and selectivities than sulfated mesoporous Ti, Amberlyst 15, HY zeolite, and H-ZSM5. Among these different pore sizes of sulfated mesoporous Nb and Ta oxides studied, $C_{12}H_2SO_4$ mesoporous Ta showed both the highest activity and selectivity, which can be attributed to its high BET surface area (292.19 $m^2 g^{-1}$), optimal pore size (18.2 Å), and increased concentration of active Brønsted acid sites on the surface of the mesoporous channels, as confirmed by ammonia TPD.

Acknowledgments

We express our gratitude to Rene Veillette for his kind help in SEM observation. Riaz Ahmad from Quantachrome is thanked for his help in TPD experiments. Professor Jichang Wang is also thanked for the analysis of thermodynamic equilibrium equation. We also acknowledge the Natural Science and Engineering Research Council of Canada (NSERC), for their financial support of this project.

Appendix A. Supplementary data

Supplementary data associated with this article can be found, in the online version, at doi:10.1016/j.jcat.2009.05.014.

References

[1] C.T. Kresge, M.E. Leonowicz, W.J. Roth, J.C. Vartuli, J.S. Beck, Nature 359 (1992) 710.
[2] J.S. Beck, J.C. Vartuli, W.J. Roth, M.E. Lernowicz, C.T. Kresge, K.D. Schmitt, C.T.W. Chu, D.H. Olson, E.W. Sheppard, S.B. Mccullen, J.B. Higgins, J.C. Schlenker, J. Am. Chem. Soc. 144 (1992) 10834.
[3] Y. Ma, W. Tong, H. Zhou, S.L. Suib, Micropor. Mesopor. Mater. 37 (2000) 243.
[4] A.K. Cheetham, G. Fe' rey, T. Loiseau, Angew. Chem. Int. Ed. 38 (1999) 3269.
[5] A. Corma, Chem. Rev. 97 (1997) 2373.
[6] D. Trong On, D. Desplantier-Giscard, C. Danumah, S. Kaliaguine, Appl. Catal. A: Gen. 253 (2003) 545.
[7] A. Taguchi, F. Schuth, Micropor. Mesopor. Mater. 77 (2005) 1.
[8] D.M. Antonelli, Y.J. Ying, Angew. Chem. Int. Ed. Engl 35 (1996) 426.
[9] D.M. Antonelli, Y.J. Ying, Chem. Mater. 8 (1996) 874.
[10] D.M. Antonelli, A. Nakahira, Y.J. Ying, Inorg. Chem. 35 (1996) 3126.
[11] M.S. Wong, D.M. Antonelli, J.Y. Ying, NanoStruct. Mater. 9 (1997) 165.
[12] D.M. Antonelli, Micropor. Mesopor. Mater. 30 (1999) 315.
[13] Z. Tian, W. Tong, J. Wang, N. Duan, V.V. Krishnan, S.L. Suib, Science 276 (1997) 926.
[14] S. Velu, M.P. Kapoor, S. Inagaki, K. Suzuki, Appl. Catal. A: Gen. 245 (2003) 317.
[15] C. Yue, M.L. Trudeau, D.M. Antonelli, Chem. Commun. (2006) 1918.
[16] C. Yue, M.L. Trudeau, D.M. Antonelli, Can. J. Chem. 83 (2005) 308.
[17] Y. Rao, M.L. Trudeau, D.M. Antonelli, J. Am. Chem. Soc. 128 (2006) 13996.
[18] J. Kang, Y. Rao, M.L. Trudeau, D.M. Antonelli, Angew. Chem. Int. Ed. 47 (2008) 1.
[19] Y. Rao, J. Kang, D.M. Antonelli, J. Am. Chem. Soc. 130 (2008) 394.
[20] J.M. Proell, E.E. Mosley, G.L. Powell, T.C. Jenkins, J. Lipid. Res. 43 (2002) 2072.
[21] B.O. Skadtchenko, Y. Rao, T.F. Kemp, P. Bhattacharya, P.A. Thomas, M. Trudeau, M.E. Smith, D.M. Antonelli, Angew. Chem. Int. Ed. 46 (2007) 2635.
[23] C. Bezouhanova, H. Lechert, G. Taralanska, A. Meyer, React. Kinet. Catal. Lett. 40 (1989) 209.
[24] M. Li, Y. Chu, H. Nie, Y. Shi, D. Li, Stud. Surf. Sci. Catal. 145 (2003) 403.
[25] F. Di-Gregorio, V. Keller, T. Di-Costanzo, J.L. Vignes, D. Michel, G. Maire, Appl. Catal. A: Gen. 218 (2001) 13.
[26] A.K. Ghosh, G. Curthoys, J. Chem. Soc. Faraday Trans. 79 (1983) 147.
[27] V. Parvulescu, S. Coman, P. Grange, V.I. Parvulescu, Appl. Catal. A: Gen. 176 (1999) 27.
[28] R. Barthos, F. Lonyi, Gy. Onyestyak, J. Valyon, J. Phys. Chem. B 104 (2000) 7311.
[29] R. Barthos, F. Lonyi, Gy. Onyestyak, J. Valyon, Solid State Ion. 141 (2001) 253.
[30] W.H. Chen, H.H. Ko, A. Sakthivel, S.J. Huang, S.H. Liu, A.Y. Lo, T.C. Tsai, S.B. Liu, Catal. Today 116 (2006) 111.
[31] P. Borges, R. Ramos Pinto, M.A.N.D.A. Lemos, F. Lemos, J.C. Vedrine, E.G. Derouane, F.R. Ribeiro, J. Mol. Catal. A: Chem. 229 (2005) 127.
[32] J.P. Joly, A. Perrard, Langmuir 17 (2001) 1538.
[33] H. Matsuhashi, K. Arata, Chem. Commun. (2000) 387.
[34] H. Matsuhashi, K. Arata, Phys. Chem. Chem. Phys. 6 (2004) 2529.
[35] F. Gaillard, J.P. Joly, A. Boreave, P. Vernoux, J.P. Deloume, Appl. Surf. Sci. 253 (2007) 5876.
[36] F. Gaillard, M. Abdat, J.P. Joly, A. Perrard, Appl. Surf. Sci. 238 (2004) 91.
[37] N.P. Bansal, J. Mater. Sci. 29 (1994) 4481.
[38] Z. Wu, Q. Wang, L. Xu, S. Xie, Stud. Surf. Sci. Catal. 142 (2002) 747.
[39] I. Eswaramoorthi, V. Sundaramurthy, N. Lingappan, Micropor. Mesopor. Mater. 71 (2004) 109.
[40] V. Logie, G. Maire, D. Michel, J.L. Vignes, J. Catal. 188 (1999) 90.
[41] S. Pariente, P. Trens, F. Fajula, F.D. Renzo, N. Tanchoux, Appl. Catal. A: Gen. 307 (2006) 51.
[42] J. Abbot, B.W. Wojciechowski, J. Catal. 90 (1984) 270.
[43] J. Abbot, B.W. Wojciechowski, J. Catal. 92 (1985) 398.